J. Fluid Mech. (2006), *vol.* 552, *pp.* 73–82.
doi:10.1017/S0022112006008615 Printed in the United Kingdom

Thermal convection in a rotating cylindrical annulus and its mean zonal flows

By J. TAO[1,2] AND F. H. BUSSE[1]

[1]Institute of Physics, University of Bayreuth, Bayreuth 95440, Germany

[2]LTCS and Department of Mechanics and Engineering Science, Peking University, Beijing 100871, P.R. China

(Received 14 July 2005 and in revised form 20 December 2005)

Thermal convection driven by centrifugal buoyancy in a rapidly rotating narrow annular channel is studied in the case of rigid cylindrical walls. The pattern of high-wavenumber thermal Rossby waves becomes increasingly modulated and finally chaotic as the Rayleigh number is increased. Retrograde as well as prograde mean zonal flows are found. The prograde mean flow dominates in fluids with large Prandtl number, while retrograde mean flows are more typical for small Prandtl numbers. Although the basic thermal Rossby waves travel in the prograde direction when the height of the annulus decreases with distance from the axis, their long-wavelength modulations often propagate in the retrograde direction.

1. Introduction

Convection driven by centrifugal buoyancy in an annular gap with conical end boundaries between a cooled inner and a heated outer cylinder rotating rigidly about their common axis has long been used as a simple model for the dynamics of convection in rotating spherical shells which is of interest for many planetary and stellar applications. In the limit of small deviations of the cones from planar surfaces, the annulus model permits a reduction of the general three-dimensional problem to a two-dimensional problem which can be analysed in terms of Cartesian coordinates when in addition the small gap approximation is used (Busse 1970, 1986). Convection starts with the onset of thermal Rossby waves travelling in the prograde azimuthal direction when the height of the annular channel decreases with increasing distance from the axis. As the Rayleigh number grows various instabilities set in, such as the mean-flow instability, the vacillation instability and others (Busse & Or 1986; Schnaubelt & Busse 1992; Brummell & Hart 1993; Abdulrahman *et al.* 2000) and finally chaotic convection arises.

Usually the problem of nearly geostrophic convection in a rotating annulus is investigated in the case of stress-free boundaries on the cylinder walls. But for comparisons with laboratory experiments it is important to take into account realistic boundary conditions on those walls. Even for applications to the problem of convection in spherical fluid shells no-slip conditions may be appropriate as for example in the region adjacent to the tangent cylinder touching the rigid inner sphere at its equator. For these reasons no-slip boundaries will be assumed in this paper.

Of particular interest in the problem of convection in a rotating annulus is the mean zonal flow generated by the Reynolds stresses of convection. This component of the velocity field appears to be rather sensitive to the boundary conditions. In

high-Rayleigh-number turbulent convection the mean zonal shear can become so strong that it disrupts the convection flow entirely. As shown in the simulations of Brummell & Hart (1993) relaxation oscillations of the mean flow component result corresponding to episodic convection. The latter occurs only for a brief period once the mean shear has decayed sufficiently due to viscous friction. During the short-lived convection bursts the Reynolds stress and thus the mean flow grow rapidly together with the amplitude of convection until the shear causes the decay of the latter. This same process has been found in simulations of convection in rotating spherical shells (Grote & Busse 2001) and it may play a fundamental role in the dynamo process since a magnetic field tends to eliminate the relaxation oscillations. For this reason it is of interest to study the relaxation oscillations in a laboratory experiment. One motivation for the analysis of this paper has thus been the question of whether relaxation oscillations can still be realized in the presence of rigid boundaries.

Another motivation has been the question of low-wavenumber instabilities of high-wavenumber rolls. The stability of high-wavenumber roll-like convection can be investigated with asymptotic methods as has been done by Abdulrahman *et al.* (2000) and others. Since those methods usually do not allow a straightforward consideration of low-wavenumber modulational instabilities it is of interest to study them numerically as will be done in this paper.

2. Basic equations and numerical methods

We consider a cylindrical annulus of average height L with the temperatures T_1 and T_2 prescribed on the inner and outer cylinders, respectively. The entire configuration is rotating rigidly with angular velocity Ω about its axis. Using the small-gap approximation with the gap width D as length scale and D^2/ν as time scale, where ν is the kinematic viscosity of the fluid and T_2-T_1 as scale of the temperature, we arrive at the following system of equations for the stream function ψ and the deviation Θ of the temperature from the purely conducting profile (see, for example, Busse 1986):

$$\left(\frac{\partial}{\partial t}+\frac{\partial}{\partial y}\psi\frac{\partial}{\partial x}-\frac{\partial}{\partial x}\psi\frac{\partial}{\partial y}-\Delta_2\right)\Delta_2\psi-\eta\frac{\partial}{\partial y}\psi+Ra\frac{\partial}{\partial y}\Theta=0, \tag{2.1a}$$

$$Pr\left(\frac{\partial}{\partial t}+\frac{\partial}{\partial y}\psi\frac{\partial}{\partial x}-\frac{\partial}{\partial x}\psi\frac{\partial}{\partial y}\right)\Theta-\Delta_2\Theta+\frac{\partial}{\partial y}\psi=0, \tag{2.1b}$$

where $\Delta_2\equiv\partial^2/\partial x^2+\partial^2/\partial y^2$ and the Rayleigh number Ra, the Prandtl number Pr and the Coriolis parameter η are defined by

$$Ra=\frac{\gamma(T_2-T_1)\Omega^2 r_0 D^3}{\nu\kappa},\quad Pr=\frac{\nu}{\kappa},\quad \eta=\frac{4\eta_0\Omega D^3}{\nu L}. \tag{2.2}$$

Here γ is the coefficient of thermal expansion, κ is the thermal diffusivity and r_0 is the mean radius of the annulus. A Cartesian coordinate system has been introduced with the x-, y- and z-coordinates oriented in the radial, azimuthal and axial directions, respectively. The term involving η arises when the equation for the z-component of vorticity, $\Delta_2\psi$, is averaged over the height of the annulus and the condition that the normal component of the velocity vanishes at the boundaries,

$$z=\pm\frac{L}{2D}\mp\eta_0 x, \tag{2.3}$$

has been taken into account together with the assumption $\eta_0\ll 1$. Through this procedure we have reduced the original equations for the three-dimensional velocity field (u, v, w) to an equation for its dominating two-dimensional geostrophic

component, $u = \partial\psi/\partial y$, $v = -\partial\psi/\partial x$, described by the stream function ψ. In order to solve (2.1) in the realistic case of no-slip cylindrical boundaries at which the conditions

$$\frac{\partial}{\partial y}\psi = \frac{\partial}{\partial x}\psi = \Theta = 0 \qquad \text{at} \quad x = \pm\tfrac{1}{2} \tag{2.4}$$

are imposed, we introduce the Galerkin representation

$$\psi = \sum_{l=1,n=0}^{\infty} (\hat{a}_{ln}(t)\cos n\alpha y + \check{a}_{ln}(t)\sin n\alpha y) f_l(x) + (4x^3 - 3x)a_{00}(t) \tag{2.5}$$

$$\Theta = \sum_{l=1,n=0}^{\infty} (\hat{b}_{ln}(t)\cos n\alpha y + \check{b}_{ln}(t)\sin n\alpha y)\sin l\pi\left(x + \tfrac{1}{2}\right) \tag{2.6}$$

where the functions $f_l(x)$ denote the Chandrasekhar functions (Chandrasekhar 1961). By adding the last term on the right hand side of (2.5), which represents the component of a Poiseuille-flow-type mean flow, we have accommodated the fact that instead of a vanishing zonal mass flux through the annulus the absence of a mean pressure gradient in the azimuthal direction must be required, satisfied when $a_{00}(t)$ obeys the equation

$$\frac{\partial}{\partial t}a_{00}(t) = -\sum_{l=even} a_{l0}(t) f_l''\left(\tfrac{1}{2}\right) - 12a_{00}(t) \tag{2.7}$$

For details we refer to earlier papers on the subject (Schnaubelt & Busse 1992; Herrmann & Busse 1998). The amplitude $a_{00}(t)$, referred to as the Poiseuille-flow coefficient in this paper, turns out to be a useful quantity for characterizing the solutions of the problem.

By projecting the equations for ψ and Θ onto the respective expansion functions, a system of ordinary differential equations for the coefficients $\hat{a}_{ln}(t)$, $\check{a}_{ln}(t)$, $\hat{b}_{ln}(t)$ and $\check{b}_{ln}(t)$ is obtained. For the numerical solution of this system of equations a truncation scheme must be introduced. We shall neglect equations and corresponding coefficients when the subscripts satisfy the inequalities $l > N_x$ and $n > N_y$, where the truncation parameters N_x and N_y must be chosen sufficiently large such that the physically relevant properties of the solution do not change significantly when N_x or N_y are replaced by $N_x - 2$ or $N_y - 2$, respectively. In order to allow for long-wavelength modulations the basic wavenumber must be chosen sufficiently small such that results obtained for a given chosen value α do not differ significantly from those obtained for $\alpha/2$. Most of the computations reported in the following have been done with $\alpha = 0.5$, $N_x = 19$ and $N_y = 144$.

In order to analyse the mean zonal flow and the temperature field, the following azimuthally averaged velocity v_0 and temperature Θ_0 are used:

$$v_0(x,t) = \frac{1}{l}\int_0^l \frac{\partial\psi}{\partial x}\,\mathrm{d}y \equiv \frac{\partial\Psi_0}{\partial x}, \quad \Theta_0(x,t) = \frac{1}{l}\int_0^l \Theta\,\mathrm{d}y, \tag{2.8}$$

where l is the periodicity length $l = 2\pi/\alpha$ and Ψ_0 is the mean stream function. In order to focus attention on the dependence of the properties of convection on the parameters R and P at high rotation rates we restrict most of the analysis to the case $\eta = 32000$.

3. Nonlinear evolution of convection and its mean flows

From weakly nonlinear analysis (Busse & Or 1986) it is known that convection in the form of thermal Rossby waves is associated with a mean flow which is symmetric

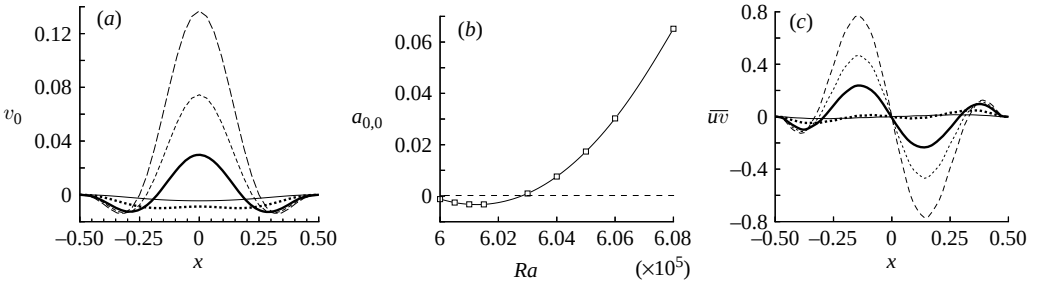

FIGURE 1. Results for $Pr = 0.71$ and $\eta = 32000$ at different Rayleigh number. (*a*) The mean velocity v_0, (*b*) the Poiseuille flow coefficient $a_{0,0}$ and (*c*) the Reynolds stress $\overline{uv}$. The thin solid curve, dark dot curve, thick solid curve, short dashed curve and long dashed curve are for $Ra = 6 \times 10^5$, 6.01×10^5, 6.03×10^5, 6.04×10^5 and 6.05×10^5, respectively.

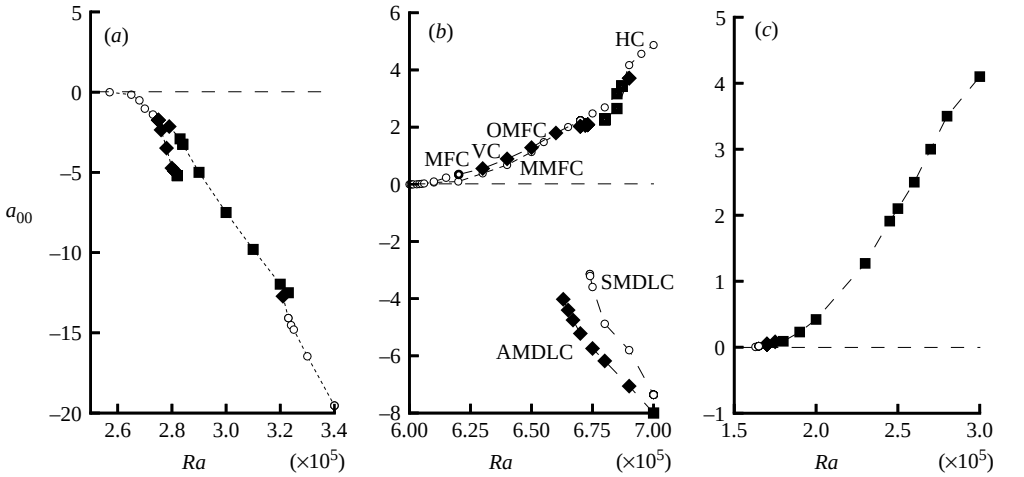

FIGURE 2. The Poiseuille-flow coefficient a_{00} for (*a*) $Pr = 0.28$, (*b*) 0.71 and (*c*) 6.7. The thin circle, thick diamond and thick square represent stationary solutions, periodic solutions and aperiodic solutions in terms of the coefficient a_{00}. For unsteady solutions a_{00} is averaged over a long time span.

with respect to the mid-plane of the channel. In the analysis of Busse & Or (1986) stress-free boundary conditions were used. But when the appropriate constant is added such that the mean flow vanishes at the boundaries it is evident that its direction is retrograde throughout the channel. This behaviour is also seen in the computations at the Prandtl number $Pr = 0.71$, as shown in figure 1. We have plotted the Poiseuille coefficient a_{00} in figure 1(*b*) since it provides a good measure for the maximum amplitude of the mean zonal flow as can be seen from comparison of figures 1(*a*) and 1(*b*). As the Rayleigh number is increased the retrograde mean zonal flow reverses to a prograde one. In order to understand this phenomenon we consider the Reynolds stress $\overline{uv}$ which generates the mean zonal flow. As shown in figure 1(*c*) the radial derivative of the Reynolds stress changes sign at the mid-plane with increasing Rayleigh number, which leads to the change of the mean velocity profile from a concave to a convex shape.

The Prandtl number dependence of the mean zonal flow is indicated in figure 2, which illustrates that solution branches with prograde and retrograde mean flows

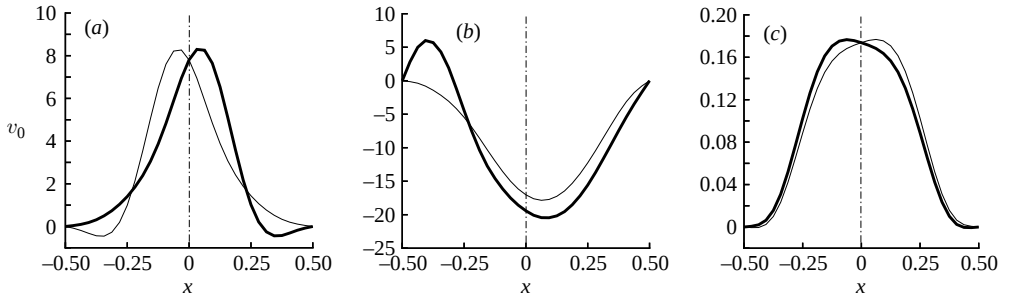

FIGURE 3. The mean velocity profiles at periodic states for (*a*) $Pr = 0.71$ and $Ra = 6.5 \times 10^5$, $\omega = 139.4$, (*b*) $Pr = 0.28$ and $Ra = 2.8 \times 10^5$, $\omega = 133.6$, and (*c*) $Pr = 6.7$ and $Ra = 1.7 \times 10^6$, $\omega = 7.4$. The solid and thick solid curves in figures are obtained at $t = 0$ and $t = \pi/\omega$, respectively.

can be found for Prandtl number of order unity. For $Pr = 0.28$ only retrograde mean flow has been found, while for $Pr = 6.7$ the mean flow is prograde in the range of Ra that has been investigated. This result contrasts with the small retrograde mean flow found in the weakly nonlinear analysis of Busse & Or (1986) for stress-free boundaries.

The branches of solutions in figure 2 show only examples of all those found in the computational simulations. Since the wavenumber $n\alpha$ of the dominant convection mode in the representation (2.5), (2.6) may vary within a finite interval at Rayleigh numbers above the critical value, numerous solutions exist for given values of the external parameters. In addition many more unstable solutions exist which, of course, could not be obtained with our computational scheme. We shall first focus on the case $Pr = 0.71$ where the most detailed investigation has been performed. The drifting symmetric thermal Rossby waves with $n = 41$ are stable only up to a value of Ra of about 6.2×10^5 where a transition to one of the two mean flow solutions (MFC) occurs (Or & Busse 1987), characterized by an asymmetric but steady mean flow profile. At the slightly higher value 6.3×10^5 of Ra the transition to vacillating convection (VC) occurs which is also known from earlier analysis for lower values of η (Schnaubelt & Busse 1992). In this form of convection the mean flow solution oscillates between its asymmetric form and a more symmetric form with the angular frequency $\omega = 87.27$. Abdulrahman *et al.* (2000) denote the two vacillating solutions by P_{a1} and $P_{a1}^{'}$. These two solutions cannot be continued beyond $Ra = 6.5 \times 10^5$ and are replaced there by a symmetrically oscillating solution which we call oscillating mean flow convection (OMFC). Abdulrahman *et al.* (2000) have denoted this solution by P_s. The oscillation of the mean flow profiles is shown in figure 3(*a*). While this type of mean flow solution was obtained for a $n = 41$ as well as $n = 40$ of the dominating mode, a different scenario develops with $n = 39$ at about $Ra = 6.4 \times 10^5$. A branch of convection called modulated mean flow convection (MMFC) appears as shown in figure 2(*b*), displayed in figure 4(*a*). In contrast to OMFC convection which alternates between the two mean flow solutions in time, MMFC convection alternates between the two mean flow solutions in space. As a consequence the mean zonal flow remains steady and symmetric. The original 'mean flows' of the two parts of the solution now correspond to circulations with the wavelength of the modulations as shown in figure 4(*b*). We call this type of convection 'stationary' because its mean properties do not change in time while the pattern propagates relative to the rigid walls. The pattern is not steady, however, even relative to a moving frame of reference since the small-scale convection and its large-scale modulation drift at different rates. In

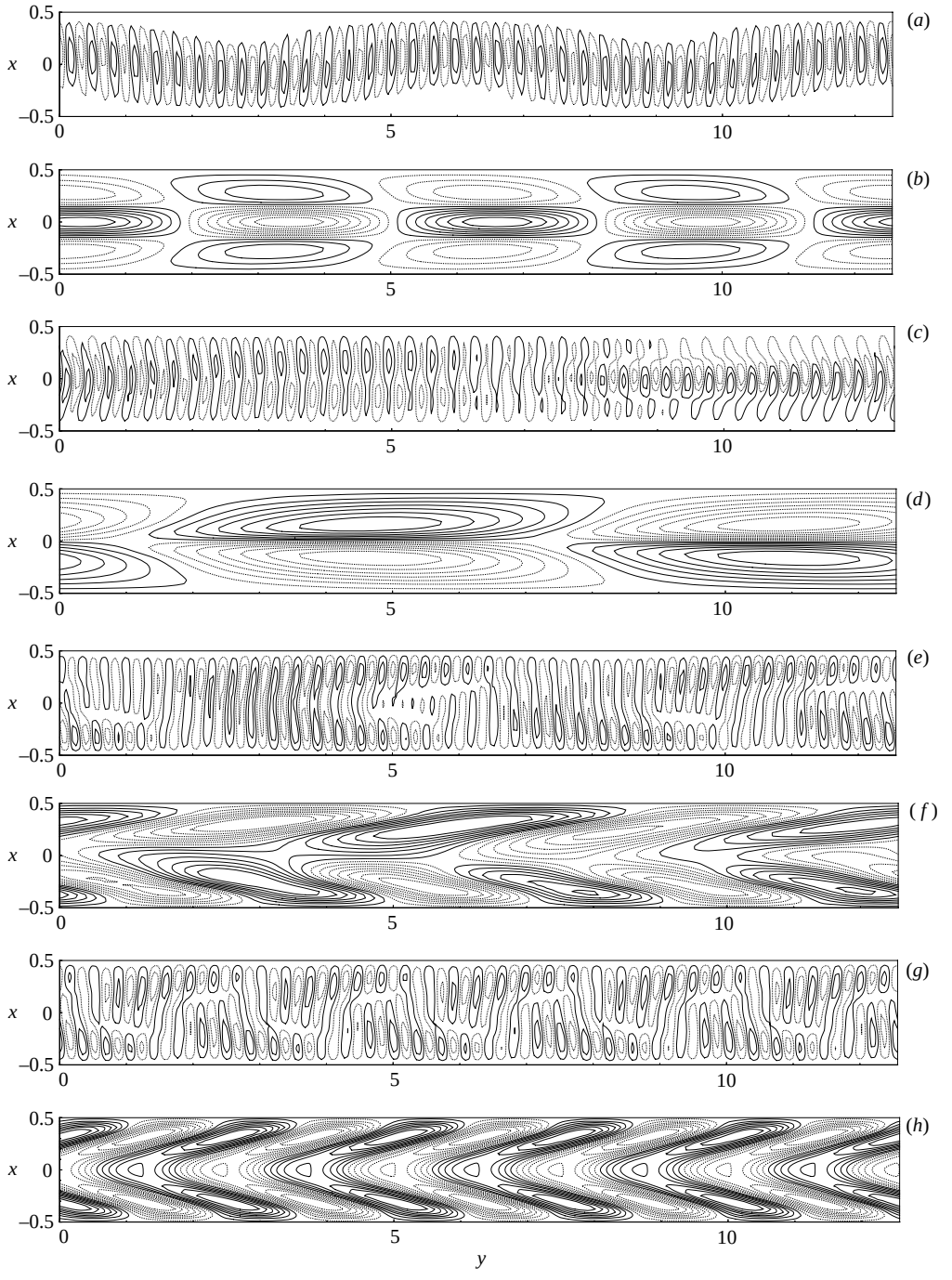

FIGURE 4. The non-axisymmetric part of the streamlines, $\psi - \Psi_0 = \text{const.}$, with (a, c) prograde mean flow and (e, g) retrograde mean flow are shown for $Pr = 0.71$. The circulation patterns corresponding to the modulation wavelength are shown in (b), (d), (f) and (h): streamlines corresponding to the terms of expression (2.5) with $n = 2, 1, 1 \leqslant n \leqslant 3$, 5 have been plotted, respectively. The Rayleigh numbers are 6.5×10^5, 7.1×10^5, 6.7×10^5 and 7×10^5 for (a, b), (c, d), (e, f) and (g, h), respectively. The corresponding velocities with which the modulations propagate are -175, 850, -288 (-174), and -190, respectively. The value in case (f) refers to the outer layer, while the value for the inner layer is given in the brackets. Solid and dotted lines indicate positive and negative values, respectively.

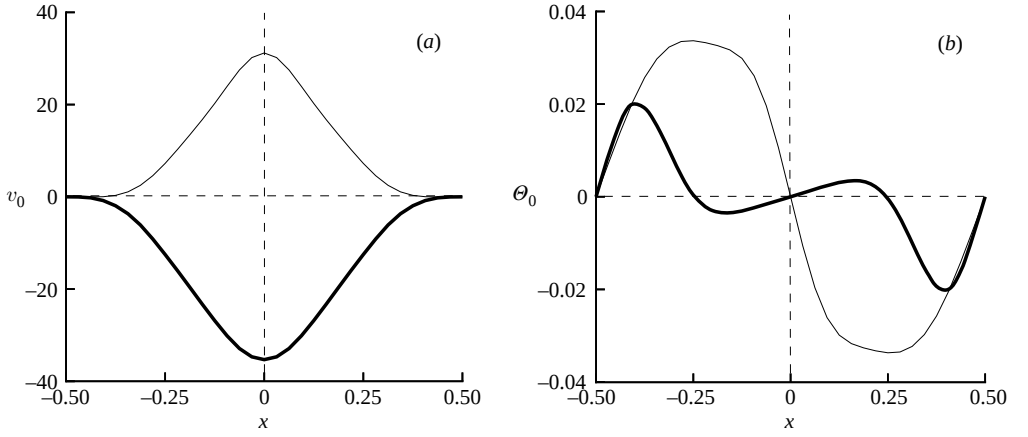

FIGURE 5. (*a*) The mean velocity profiles and (*b*) the mean temperature profiles of stationary solutions for $Pr = 0.71$. The thick solid line is for $Ra = 7 \times 10^5$(SMDLC), and the thin solid line is for 7.1×10^5(HC convection).

all cases except figure 4(*d*) the modulations propagate in the retrograde direction with relatively high phase velocities of the order 200. This value is not only large in comparison to the maximum absolute value of the mean zonal flow, but also exceeds the group velocity of the thermal Rossby waves.

As the Rayleigh number is increased further, solutions with time-periodic and aperiodic Nusselt number appear. But at still higher values of Ra stationary forms of convection reappear. These solutions are characterized by the combination of single-layer and double-layer convection as shown in figure 4(*c*). We call this pattern hybrid convection (HC). In addition to the prograde mean zonal flow an alternating large-scale circulation exists as indicated in figure 4(*d*).

For the branches with retrograde mean zonal flow we also observe double-layer convection. But the modulations of the outer and inner parts are no longer necessarily correlated as the example of figure 4(*e*) demonstrates. Here an $\alpha = 1$ modulation coexists with an $\alpha = 1.5$ modulation. Since the drifts of the outer and inner parts are no longer synchronous the solution becomes time periodic. We shall call this type of convection asynchronously modulated double-layer convection (AMDLC). The mean flow for this type of convection is slightly asymmetric and oscillates a little. Often, of course, the modulations of the inner and outer parts of the double layer have the same wavenumber such that a stationary drifting pattern of convection is obtained as shown in figure 4(*g*). This kind of convection will be called synchronously modulated double-layer convection (SMDLC). The profiles of the mean zonal flow and of the mean temperature of this type of convection are shown by the thick lines in figure 5. The large-scale circulation patterns for AMDLC and SMDLC are shown in figures 4(*f*) and 4(*h*), respectively.

Besides the stationary and time-periodic solutions, quasi-periodic and chaotic solutions are found, especially at higher Rayleigh numbers beyond about 8×10^5. Examples for the time dependence of the Nusselt number are shown in figure 6. But the spatial structure of these solutions is difficult to characterize without a large number of plots. It appears that a combination of large-scale and small-scale changes occurs in the structure of convection. These changes may correspond to the bifurcations studied by Abdulrahman *et al.* (2000) in their asymptotic analysis of the small-scale convection

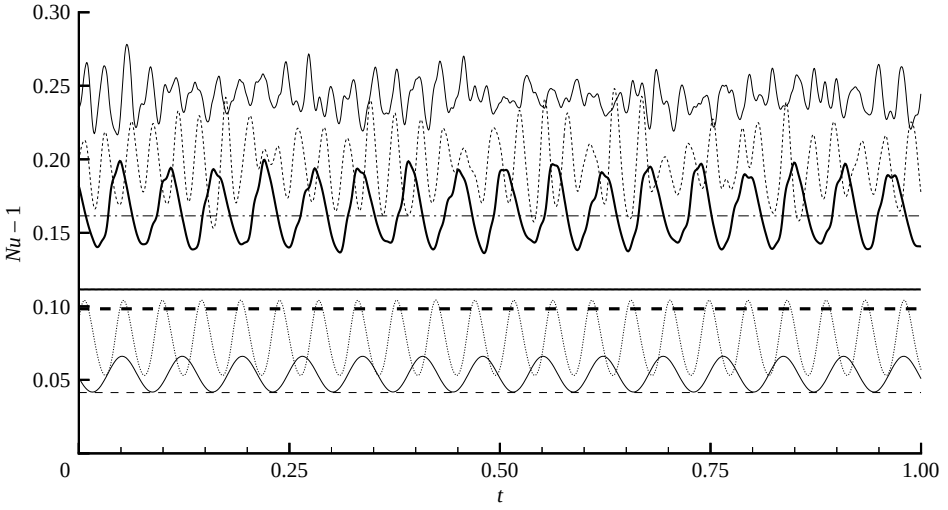

FIGURE 6. Nusselt number Nu as a function of time t for $Pr = 0.71$ at different Rayleigh numbers for the case of prograde mean flow. The Rayleigh numbers for the curves from bottom to top are 6.2×10^5, 6.3×10^5 (VC), 6.5×10^5 (OMFC), 6.6×10^5 (MMFC), 6.7×10^5 (MMFC), 7.1×10^5 (dashed-dotted line, HC), 7.17×10^5, 7.5×10^5 and 8×10^5, respectively.

rolls. But through the additional frequencies introduced by the large-scale modulations a much more complex time-dependence is obtained.

For $Pr = 0.28$ the thermal Rossby waves typically set in with $n = 33$ and are soon replaced by a modulated stationary solution of the hybrid type as Ra increases beyond its critical value. The streamline pattern thus resembles that of figure 4(c). As in the latter case the modulation corresponds to the wavenumber $\alpha = 0.5$ and travels in the prograde direction. For $Ra = 2.68 \times 10^5$ the speed reaches 625.

As the Rayleigh number is further increased two types of time-periodic solutions can be found. In both cases the solutions are asymmetric, i.e. there exist two forms of the solutions which obey reflection symmetry with respect to the mid-plane of the layer. For the lower values of a_{00} in figure 2(a) the convection flow switches periodically between a state close to the original Rossby waves and the mean flow solution in which convection is concentrated towards one side of the channel (Or & Busse 1987). This solution thus corresponds to vacillating convection (Schnaubelt & Busse 1992) except that a slight modulation with $\alpha = 0.5$ is present. Accordingly, the mean flow profile is asymmetric as shown in figure 3(b).

For the higher values of a_{00}, i.e. smaller $|a_{00}|$, there are two dominant modes corresponding to wavenumbers $n\alpha$ with $n = 32$ and 33. The hybrid type of convection becomes periodically stronger in this case on one side of the channel which again leads to an asymmetric mean flow similar to the one shown in figure 3(b), but with a smaller amplitude and lower frequency of $\omega = 83.5$ at $Ra = 2.79 \times 10^5$. The modulation with $\alpha = 0.5$ is much stronger in this case as follows from the interference of the two dominant modes.

As the Rayleigh number reaches values of the order of 3.2×10^5 the convection returns to a symmetric stationary form of the type SMDLC that has been discussed above and is illustrated in figures 4(g) and 4(h). The modulation wavenumber tends to be somewhat larger than for $Pr = 0.71$, but the retrograde propagation speed of the modulation is of the same order. For $Ra = 3.4 \times 10^5$ its value is -250.

For $Pr = 6.7$ a direct transition from thermal Rossby waves into a modulated time-periodic state of convection occurs. This state is similar to the state SMDLC with the

amplitude increasing and decreasing periodically on one side of the channel or the other. Accordingly, the profile of the mean flow also changes periodically between its two extreme positions as indicated in figure 3(*c*). With increasing *Ra* the periodic convection state soon changes into an aperiodic one as indicated in figure 2(*c*).

4. Concluding discussion

The analysis of § 3 has demonstrated that a rather rich scenario of spatio-temporal patterns is obtained for centrifugally driven convection in a rapidly rotating cylindrical annulus. The presence of rigid cylindrical walls somewhat suppresses the mean zonal flow such that the relaxation oscillations of the stress-free case (Brummell & Hart 1993) have not been found. Note that the relaxation oscillations are also suppressed when the sidewalls are still stress-free, but the conical end surfaces are rigid such that Ekman layer suction tends to damp the mean shear as in the annulus problem treated by Jones, Rotvig & Abdulrahman (2003). The various forms of modulations identified in the present paper are of considerable interest, however, and should be an attractive subject for a laboratory investigation. Because of the loss of symmetry with respect to the mid-plane in experimental configurations, some of the bifurcations mentioned in this paper will become imperfect. But the variety of patterns should still be observable when the small gap annulus is approximated.

The basic small-scale convection rolls are not strongly influenced by the nature of the boundary conditions at high values of η. But the mean flow and some of the modulational instabilities are affected. Nevertheless, SMDLC convection compares well with the pattern that Brummell & Hart (1993) obtained for stress-free walls in their figure 9(*f*). However, the 'double layer' patterns corresponding to their figure 6 could be obtained in the present computations only for $\alpha \geqslant 1$ in agreement with the value $\alpha = 1$ used by Brummell & Hart (1993). The 'double-layer' convection disappeared when α is lowered to 0.5.

The computational study of this paper is restricted by the lowest value of α for which solutions with sufficiently high numerical resolution can be obtained. In some cases it is evident that the modulation instability with the lowest possible value of α will occur first. This is also evident when results obtained for $\alpha = 0.25$ shown in figure 7 are compared with those obtained for $\alpha = 0.5$ shown in figure 6. Except for minor quantitative differences the solutions obtained for the two values of α are the same and the sequence of transitions remains unchanged. Quasi-periodic and chaotic solutions usually occur at lower values of *Ra* for $\alpha = 0.25$ than for $\alpha = 0.5$ as expected since this replacement doubles the number of degrees of freedom of the system.

Sometimes a branch of solutions obtained for a higher value of α disappears altogether when α is lowered as has been noted above. Another example is found for $Pr = 0.28$. Here a branch of stationary solutions with prograde mean flow was found with $\alpha = 2.0$ for $Ra \geqslant 3.3 \times 10^5$. But this branch became unstable and switched to the solutions with retrograde mean flow when α was halved.

An unexpected result is that the pattern sometimes changed from a periodic one to a stationary one or from a quasi-periodic one to a periodic one when α was replaced by $\alpha/2$. Since this replacement doubles the number of degrees of freedom of the system the opposite change might have been expected. But, apparently, the increased number of degrees of freedom can also facilitate the transition of convection to its optimal state.

Finally we note that computations have been extended to the case $\eta = 24000$ for $Pr = 0.71$ in order to demonstrate that the results reported in this paper are indeed representative for the case of high η. All the branches referred to in figure 2(*b*) have been found in that case as well, but the frequencies and the modulation wavelengths

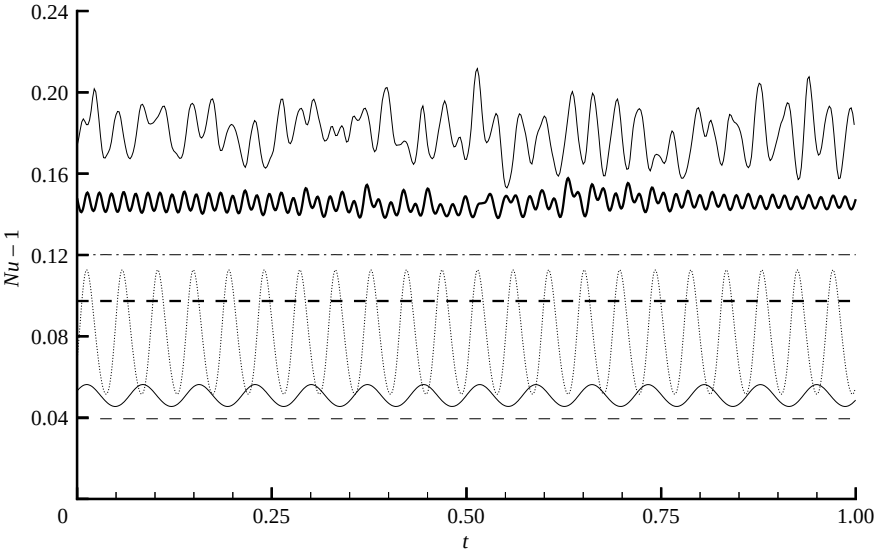

FIGURE 7. Nusselt number Nu as a function of t for $Pr = 0.71$ at different Rayleigh number for the branch with prograde mean flow calculated with half the α value used in figure 6. The curves from bottom to top correspond to $Ra = 6.2 \times 10^5$, 6.3×10^5 (VC), 6.5×10^5 (OMFC), 6.6×10^5 (MMFC), 6.8×10^5 (HC), 7.0×10^5 and 7.5×10^5, respectively.

are lower. The onset of thermal Rossby waves occurs at $Ra = 4.15 \times 10^5$ and the branch with prograde mean flow follows the same sequence of transitions as indicated in figure 2(b). The frequency of vacillation starts with $\omega = 55.6$ and assumes the value $\omega = 96.6$ for the OMFC-solution at $Ra = 4.4 \times 10^5$. Branches with retrograde mean flow also exist. The SMDLC-solution at its onset at $Ra = 4.8 \times 10^5$ is now characterized by a modulation wavenumber of 3.5 and a drift rate of -100 instead of the values 2.5 and -190 as in the case of figure 4(g, h).

This work is partially supported by the A.-v.-Humboldt Foundation. Professor Werner Pesch's helpful suggestions are appreciated by the authors.

REFERENCES

ABDULRAHMAN, A., JONES, C. A., PROCTOR, M. R. E. & JULIEN, K. 2000 Large wavenumber convection in the rotating annulus. *Geophys. Astrophys. Fluid Dyn.* **93**, 227–252.

BRUMMELL, N. H. & HART, J. E. 1993 High Rayleigh number β-convection. *Geophys. Astrophys. Fluid Dyn.* **68**, 85–114.

BUSSE, F. H. 1970 Thermal instabilities in rapidly rotating systems. *J. Fluid Mech.* **44**, 441–460.

BUSSE, F. H. 1986 Asymptotic theory of convection in a rotating cylindrical annulus. *J. Fluid Mech.* **173**, 545–556.

BUSSE, F. H. & OR, A. C. 1986 Convection in a rotating cylindrical annulus. Part 1. Thermal rossby waves. *J. Fluid Mech.* **166**, 173–187.

CHANDRASEKHAR, S. 1961 *Hydrodynamic and Hydromagnetic Stability*. Oxford University.

GROTE, E. & BUSSE, F. H. 2001 Dynamics of convection and dynamics in rotating spherical fluid shells. *Fluid Dyn. Res.* **28**, 349–368.

HERRMANN, J. & BUSSE, F. H. 1998 Stationary and time dependent convection in the rotating cylindrical annulus with modulated height. *Phys. Fluids* **10**, 1611–1620.

JONES, C. A., ROTVIG, J. & ABDULRAHMAN, A. 2003 Multiple jets and zonal flow on Jupiter. *Geophys. Res. Lett.* **30**, 1731.

SCHNAUBELT, M. & BUSSE, F. H. 1992 convection in a rotating cylindrical annulus, part 3. vacillating and spatially modulated flows. *J. Fluid Mech.* **245**, 155–173.